INTERROGATION OF NUMERICAL SIMULATION FOR MODELING OF FLOW INDUCED MICROSTRUCTURE

Daniel D. Joseph
Department of Aerospace Engineering and Mechanics
University of Minnesota
Minneapolis, Minnesota

Published in *ASME FED* **189** (Liquid-Solid Flows), 31-40 (1994).

ABSTRACT

This paper summarizes our recent efforts using direct numerical simulations to determine microstructural properties of fluidized suspensions of a few particles. We have been studying the motions of a few particles in a viscous fluid by direct numerical simulation at moderate values of the Reynolds number in the 100's. From these simulations, we find the mechanisms which give rise to lateral migration of particles and turn the broad side of long bodies perpendicular to the stream. We find that a viscous "stagnation" point is a point on the body where the shear stress vanishes and the pressure is nearly a maximum. We show how the migration is controlled by stagnation and separation points and go further than before in the discussion of Segré-Silberberg effects of cross-streamline migration in two dimensions. We have analyzed the lift off and steady flight of solid capsules in Poiseuille flows. We do a three-dimensional simulation of steady flow at slow speeds and show that the extensional stresses in a viscoelastic flow change the sign of the normal stress which would exist at points of stagnation in a Newtonian fluid, causing the long side of the body to line up with the stream.

INTRODUCTION

This paper is a review of CFD approaches to problems of two-phase flows which have been developed by my colleagues and ex-students, H. Hu and P. Singh, my present students, J. Feng, T. Hesla and Y. Huang, and my colleagues, M. Crochet, R. Glowinski and T. Pan. Our goal is to obtain exact results in which the nonlinear hydrodynamic mechanisms inducing flow microstructure are fully revealed. We have determined the motion of a few interacting particles in a variety of flows at Reynolds numbers up to the hundreds. Most, but not all, of our simulations have been restricted to two dimensions. Direct simulations of the motion of many particles, even in two dimensions, have not yet been done. Stokesian dynamics is an approximate and not direct numerical method of handling the motion of many particles when inertia of the fluid and inertia of the particle are neglected. By interrogating our simulations, we are able to identify the nonlinear mechanisms which produce microstructures through particle-particle and wall-particle interactions. Microstructural properties of fluidized suspensions in Newtonian fluids are associated with wake interactions and turning couples on long bodies in a scenario, which I have described as drafting, kissing and tumbling. Kissing particles are sucked together in wakes and the long body, which kissing spheres momentarily form, is unstable when the axis of the long body is along the stream. The kissing spheres tumble into across-the-stream arrangements basically for the same reason that a long body will put its broadside perpendicular to the stream. These microstructural elements endow a fluidized suspension with anisotropic structure in which spherical particles on the average line up across the stream. The anisotropy, which is readily observed in experiments, is due to nonlinear mechanisms revealed in simulations that could not be predicted by any of the continuum models of two-phase flows or even by perturbation methods which were promoted in the 1980's.

Other features of particle-fluid, particle-particle and particle-wall interactions which can be illuminated by intelligent interrogation of direct simulations are related to the effects of the shear and pressure distributions exerted by the fluid on the particle surface on the motion of the particle. These forces are responsible for lateral drift and rotation of particles in sedimenting and shear flows. We can determine the effects of the walls on the equilibrium position of the particles away from the wall. We can also study the evolution of systems of particles as dynamical systems by looking at the bifurcations of steady solutions.

We have developed two types of direct finite-element simulations in which the forces exerted by the fluid on the body are computed. The first type of calculation can be called a force calculation and the second is a motion calculation. In a force calculation, the position and velocity of the bodies are prescribed and the fluid motion is computed by a Navier-Stokes solver. We have used three kinds of solvers and they all work well. After having computed the fluid motion, we can compute the forces and moments that are exerted by the fluid on the objects in the flow. The forces tell us how the body would move thereafter if it could. In a motion calculation, we actually move the body with those forces and carry out a motion simulation iteratively. Of course, we like motion calculations better because they go further. The only force calculations we have done are described in the paper by Singh, Caussignac, Fortes, Joseph and Lundgren [1989], which was our first CFD effort, and the paper by Feng, Joseph, Glowinski and Pan [1993], which was our first three-dimensional CFD effort. All the other papers are motion calculations that extend and enhance a finite-element package first introduced by Hu, Joseph and Crochet [1992].

In this paper, I will give an overview of our works on direct simulations of two-phase flows emphasizing the intelligent interrogation of simulations for the underlying fluid dynamics rather than the details of algorithm development. I will follow a chronological format in presenting the results, listing the abstract of each paper verbatim, followed by a selection of some special results designed to give the reader the flavor of the work. We have actually done quite a lot and much of it is not yet published.

SELECTED WORKS

1. Singh, P. Caussignac, P.H., Fortes, A., Joseph, D.D. and Lundgren, T., 1989, "Stability of Periodic Arrays of Cylinders Across the Stream by Direct Simulation," *J. Fluid Mech.* **205**, pp. 553-571.

   We treat the problem of the stability of an infinite horizontal array of cylinders, spaced periodically, by a direct numerical simulation of the Navier-Stokes equations for steady flow at Reynolds numbers less than or equal to 100. We find that the only stable configuration for the array is one with equal spacing between cylinders and all cylinders lying on a line perpendicular to the flow. The array is found to be stable under displacements of the cylinders perpendicular and parallel to the array. We say a perturbation is stable when it gives rise to a force which acts to restore the original stable configuration. Our results are consistent with experiments in which spheres were confined by the sidewalls of a fluidized bed to move in two dimensions. As a secondary issue we consider the variation with parameters of the length and width of wakes behind cylinders.

This paper may have been the first to give the results of direct simulation of flow at finite Reynolds numbers past an array of cylinders in which no assumption is made about the nature of the flow near the cylinders. The stability calculation is also the first of its type and the results are satisfactory. One defect of the calculation is that a too strong interpretation of periodicity is used in which it is assumed that vertical lines between the spheres are streamlines.

2. Hu. H.H., Joseph, D.D. and Crochet, M., 1992, "Direct Simulation of Fluid Particle Motions," *Theoretical and Computational Fluid Dynamics* **3**, pp. 285-306.

   Continuum models of two phase flows of solids and liquids use constitutive assumptions to close the equations. A more fundamental approach is a "molecular dynamic" simulation of flowing "big" particles based on reliable macroscopic equations for both solid and liquid. We developed a package that simulates the unsteady two dimensional solid-liquid two phase flows using the Navier-Stokes equations for the liquid and the Newton's equations of motion for the solid particles. The Navier-Stokes equations are solved using a finite element formulation and the Newton's equations of motion are solved using an explicit-implicit scheme. We show that the simplest fully explicit scheme to update the particle motion using Newton's equations is unstable. To correct this instability we propose and implement an Explicit-Implicit Scheme in which at each time step, the positions of the particles are updated explicitly, the computational domain is remeshed, the solution at the previous time is mapped onto the new mesh, and finally the non-linear Navier-Stokes equation and the implicitly discretized Newton's equations for particle velocities are solved on the new mesh iteratively. The numerical simulation reveals the effect of vortex shedding on the motion of the cylinders and reproduces the drafting, kissing and tumbling scenario which is the dominant rearrangement mechanism in two-phase flow of solids and liquid in beds of spheres which are constrained to move in only two dimensions.

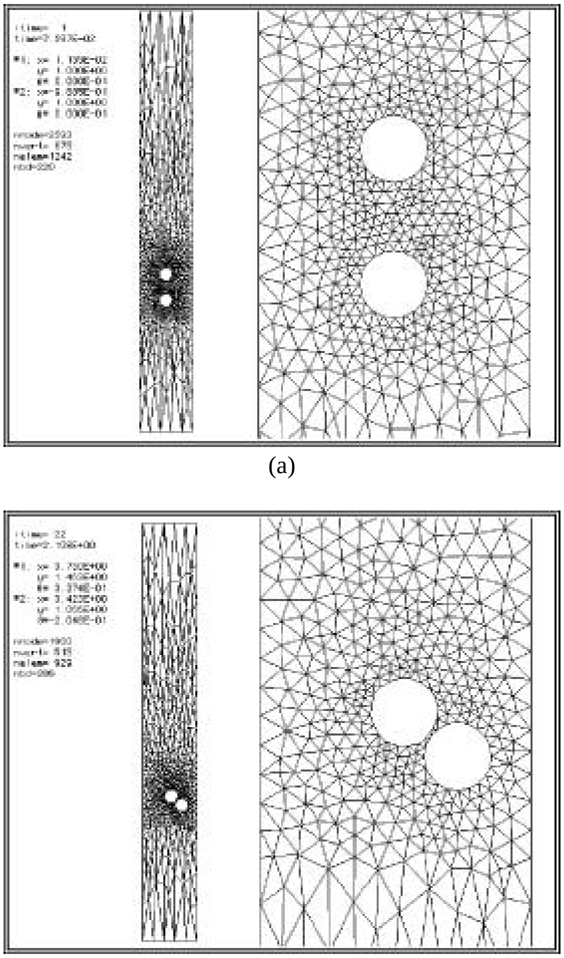

(a)

(b)

Figure 1. Some typical meshes used in the computation. In each window, the left is an overall view of the mesh and the right is a closer view near the cylinders. The core of our remeshing package is the subroutine MSHPTG from the interactive two-dimensional mesh generator EMC2 developed by F. Hecht and E. Saltel [1989]. The remeshing package has a refinement capability in the regions where the cylinders are very close to the channel walls, as in (b).

This was the first paper in which we moved the particles in a full dynamical simulation. The Navier-Stokes equations are solved using a finite element code POLYFLOW (Crochet, Debaut, Keunings and Marchal, [1991]). The dynamic coupling between the fluid flow and the motion of the particles is realized by an Explicit-Implicit scheme developed in the paper.

The numerical simulation involves three major difficulties. The first is automatic remeshing. We use unstructured meshes since the geometry of the computation domain can change drastically from time to time. A new mesh needs to be generated at each time, according to the positions of the particles. Some typical meshes are shown in Figure 1.

The second difficulty is projection. The flow field at the old time step must be mapped onto the new mesh in order to evaluate the unsteady term in the Navier-Stokes equations in Eulerian form. Finally, the numerical scheme that discretizes the coupled Navier-Stokes equations and particle equations has to be stable and efficient.

The basic procedure is as follows:

(1) Explicit updating. At time t_i, the current position, velocity of and force on the particle are used to predict the new position and velocity at time t_{i+1}.

(2) Remeshing and projection. For this new position, the computational domain is remeshed and the velocity field at t_i is projected onto the new mesh.

(3) Navier-Stokes solution. On the new mesh, the pressure and velocity fields at t_{i+1} are computed using the velocity field at t_i (after projection). The explicitly updated particle velocity serves as the boundary condition on the particle surface. Then the force and moment on the particle are computed.

(4) Implicit updating. The velocity of the particle is re-updated implicitly using the force and moment at t_{i+1}. If the new particle velocity is different from the one obtained in (1), then we go back to (3) and solve the Navier-Stokes equations using the new particle velocity as the boundary condition. This process is repeated until satisfactory convergence is reached.

In POLYFLOW, the surface force on the solid particle is not integrated directly from the stress tensor on boundary nodes. Instead, the Gauss integral formula is used to convert this surface integral into a volume integral on the domain outside the particle. This method of computation does not give the distributions of surface stresses. Huang, Feng and Joseph [1993, number 5 in this list] enhanced the motion solver with a package which computes the shear stress on the body directly from the velocity gradient in the finite elements around the capsule. The pressure force is obtained from the pressure field which is computed from POLYFLOW without enhancement.

3. Hu, H., Joseph, D.D. and Fortes, A., 1992, "Experiments and Direct Simulations of Fluid Particle Motion," *Int. Video J. of Eng. Res.* **2,** pp. 17-24.

This paper and the accompanying video segment show how the motions of sedimenting particles may be simulated by direct computations based on the Navier-Stokes equations and the particles equations of motion. Sedimenting and fluidized particles are confined by closely spaced walls to move essentially in two dimensions under forces determined by three-dimensional motions of the fluidizing liquids. Attention is confined to the case when there are only few particles, not more than four. The experiments and simulations give rise to deterministic dynamics, to equilibrium positions and steady flows, to Hopf bifurcation and wavy fall trajectories and to more *chaotic motions. It is shown that long bodies always turn to put their broadside perpendicular to the stream. The same mechanism which causes long bodies to turn broadside-on causes spherical bodies, which come into contact by wake interactions, to tumble, giving rise to a flow induced anisotropy in which across stream arrangements are favored. The numerical simulation, unlike the experiments, is strictly two-dimensional, but many of the observed features of the experiments are predicted by the simulation.*

The video segment on which this paper is based is a stand alone document. The paper gives additional information which is not conveniently expressed in a video format.

4. Hu, H.H. and Joseph, D.D., 1994, "Evolution of a Liquid Drop in a Spinning Drop Tensiometer," *J. Colloid and Interface Science* **162**, pp. 331-339.

To obtain desired material properties, a blend of two mostly incompatible polymers is often used. The blend morphology developed during the mixing process of molten polymers is strongly influenced by interfacial tension between the polymers. A spinning drop tensiometer is commonly used to measure the interfacial tension between two polymeric liquids. In this study a numerical method is developed which simulates the evolution of a liquid drop in a spinning drop apparatus. The Navier-Stokes equations are solved with a finite element formulation. A mixed Lagrangian and Eulerian technique is used to deal with the moving interface. The computation domain is remeshed and the flow field is interpolated to avoid mesh entanglement as drop deforms. The simulation generates the relaxation curves for the radius and the length of the drop. The numerical results show that the shear stress on the drop surface is quite important. A simple theory of relaxation is then formulated which takes account of the shear stress on the surface of the cylindrical drop. It is found that the exponent for the relaxation of the drop depends on the interfacial tension, the equilibrium radius of the drop, the viscosities of both fluids and the geometric ratios of the length to the radius of the drop and of the radius of the container to the radius of the drop.

5. Liu, Y.J., Nelson, J., Feng, J. and Joseph, D.D., 1993, "Anomalous Rolling of Spheres Down an Inclined Plane," *J. Non-Newtonian Fluid Mech.* **50,** pp. 305-329.

A sphere in air will roll down a plane that is tilted away from the vertical. The only couple acting about the point of contact between the sphere and the plane is due to the component of the weight of the sphere along the plane, provided that air friction is negligible. If on the other hand the sphere is immersed in a liquid, hydrodynamic forces will enter into the couples that turn the sphere, and the rotation of the sphere can be anomalous, i.e., as if rolling up the plane while it falls. In this paper we shall show that anomalous rolling is a characteristic phenomenon that can be observed in every viscoelastic liquid tested so far. Anomalous rolling is normal for hydrodynamically-levitated spheres, both in Newtonian and viscoelastic liquids. Normal and anomalous rolling are different names for dry and hydrodynamic rolling. Spheres dropped at a vertical wall in Newtonian liquids are forced into anomalous rotation and are pushed away from the wall while in viscoelastic liquids, they are forced into anomalous rotation, but are pushed towards the wall. If the wall in inclined and the fluid is Newtonian, the spheres will rotate normally for dry rolling, but the same spheres rotate anomalously in viscoelastic liquids when the angle of inclination from the vertical is less than some critical value. The hydrodynamic mechanisms underway in the settling of circular particles in a Newtonian fluid at a vertical wall are revealed by an exact numerical simulation based on a finite-element solution of the Navier-Stokes equations and Newton's equations of motion for a rigid body.

The numerical simulation is restricted to the case in which a circular particle is dropped in a Newtonian fluid at a vertical wall. In our experiments, spheres dropped from rest in glycerin would rotate and drift rapidly away from the wall and after a short time reach an apparently steady state with a definite angular velocity w_0 and a fixed stand-away distance with no further side drift. In the simulation, the particle is seen to drift to the center of the channel, and the drift takes place on a much larger time scale. The rotation of the particle is anomalous at the beginning, and dies away as the particle approaches its equilibrium position at the channel center.

At first, when the particle is very near the wall, the passage of fluid between the circular particle and the wall is blocked, so that the flow passes over the outside of the circular particle, turning it in the direction that we call "anomalous." The pressure and shear stress distributions on the surface of the particle shows that the maximum pressure occurs roughly at the point of vanishing shear stress (Figure 2).

In Figure 3 we have compared the side thrusts, p sin$q$ of the pressure and $\tau \cos q$ of the shear stress on the boundary $a = 0$ of the circular particle. The side force resultants of these stresses are given by integration over q

$$
\begin{aligned}
[F_p, F_t] &= \int_0^{2p} [p \sin q,\ t\ \cos q]\, a\, dq \\
&= [-0.062,\ 0.013]\ \text{dyne cm}^{-1} \qquad (1)
\end{aligned}
$$

The lateral thrust of the pressure gives rise to the largest contribution to the total thrust. The lateral thrust of the shear stress opposes the thrust due to pressure.

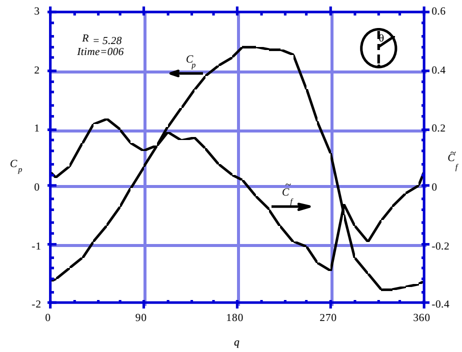

Figure 2. Pressure and shear stress distribution on a circular particle, at R = 5.28, in terms of dimensionless coefficients $C_p = 2p/rU^2$ and $C_f = 2t_{rq}/rU^2$ where U is the falling speed. The modified stress distribution $\tilde{t}_{rq}$ is expressed through the modified coefficient $\tilde{C}_f$. Because the angular speed is small, the difference between $\tilde{C}_f$ and C_f is only about 0.3% and cannot be seen in this plot. The maximum pressure is very near the "stagnation" point where the modified shear stress vanishes ($\tilde{C}_f$ = 0) on the front face of the circle.

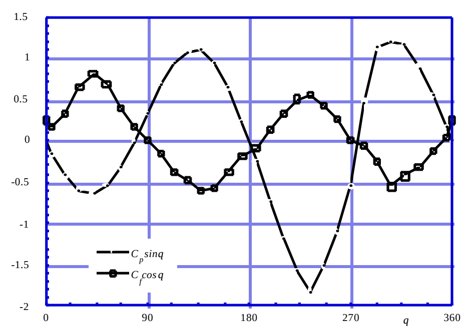

Figure 3. Distributions of the side thrust coefficients for the pressure C_p sin*q*, for the viscous part of the normal stress C sin*q* and for the shear stress C_f cos*q* on the surface of a circular particle settling near a wall with R = 5.28 and $x/d = 10^{-3}$. The resultant side thrusts are given by (1). The lateral thrust of the pressure gives rise to the largest contribution of the total thrust. The lateral thrust of the shear stress opposes the thrust of the normal stress due to pressure.

In Figure 3 we have compared the side thrusts, *p* sin*q* of the pressure and τ cos*q* of the shear stress on the boundary *a* = 0 of the circular particle. The side force resultants of these stresses are given by integration over *q*

$$\begin{aligned}\left[F_p, F_t\right] &= \int_0^{2p} \left[p \sin q,\ t \cos q\right] a\, dq \\ &= \left[-0.062,\ 0.013\right] \text{dyne cm}^{-1} \qquad (1)\end{aligned}$$

The lateral thrust of the pressure gives rise to the largest contribution to the total thrust. The lateral thrust of the shear stress opposes the thrust due to pressure.

After the particle drifts sufficiently far away from the wall, the blockage is relieved and a more symmetrical flow pattern is achieved. The pressure and shear stress on the circle resemble those on a fixed particle in a uniform flow, and the rotation and lateral drift eventually vanish.

6. Feng, J., Hu, H.H. and Joseph, D.D., 1994, "Direct Simulation of Initial Value Problems for the Motion of Solid Bodies in a Newtonian Fluid. Part 1: Sedimentation," *J. Fluid Mech.* **261,** pp. 95-134.

This paper reports the result of direct simulations of fluid-particle motions in two dimensions. We solve the initial value problem for the sedimentation of circular and elliptical particles in a vertical channel. The fluid motion is computed from the Navier-Stokes equations for moderate Reynolds numbers in the hundreds. The particles are moved according to the equations of motion of a rigid body under the action of gravity and hydrodynamic forces arising from the motion of the fluid. The solutions are as exact as our finite element calculations will allow. As the Reynolds number is increased to 600, a circular particle can be said to experience five different regimes of motion: steady motion with and without overshoot and weak, strong and irregular oscillations. An elliptic particle always turns its long axis perpendicular to the fall, and drifts to the center-line of the channel during sedimentation. Steady drift, damped oscillation and periodic oscillation of the particle are observed for different ranges of the Reynolds number. For two particles which interact while settling, a steady staggered structure, a periodic wake-action regime and an active drafting-kissing-tumbling scenario are realized at increasing Reynolds numbers. The non-linear effects of the particle-fluid, particle-wall and inter-particle interactions are analyzed, and the mechanisms controlling the simulated flows are shown to be lubrication, turning couples on long bodies, steady and unsteady wakes and wake interactions. The *results are compared to experimental and theoretical results previously published.*

7. Huang, P.Y., Feng, J. and Joseph, D.D., 1994, "The Turning Couples on an Elliptic Particle Settling in a Vertical Channel," *J. Fluid Mech.* (in press).

We do a direct two-dimensional finite element simulation of the Navier-Stokes equations and compute the forces which turn an ellipse settling in a vertical channel of viscous fluid in a regime in which the ellipse oscillates under the action of vortex shedding. Turning this way and that is induced by large and unequal values of negative pressure at the rear separation points which are here identified with the two points on the back face where the shear stress vanishes. The main restoring mechanism which turns the broadside of the ellipse perpendicular to the fall is the high pressure at the "stagnation point" on the front face, as in potential flow, which is here identified with the one point on the front face where the shear stress vanishes.

To do this interrogation we had to enhance the code so that the separate contributions of the shear stress and pressure to the force and moment on the body could be computed. Hu et al. [1992] calculated the pressure and the total force in an indirect manner which did not allow us to interrogate the results. First we found that the viscous part of the normal stress vanishes at each point on the boundary; in the plane tangent to a rigid body at the point in question, tangential derivatives of the velocity vanish and the continuity equation then shows that the normal derivative of the normal velocity also vanishes. This implies that $D_{nn} = 0$. This is an obvious result which must be known, though we could not find it in the literature. Of course, everyone knows that to compute the drag, you need the shear stress and pressure. Second, we found that a viscous "stagnation" point is a point on the body where the shear stress vanishes and the pressure is nearly a maximum. Separation points are also stagnation points in the sense of vanishing shear stress, but the pressures are minimum there. The computation showed that the pressures turn the body, with pressures at the separation points turning the body to and fro at successive vortex shedding events, and the stagnation pressures always resist turning, producing couples which turn the long axis of the ellipse perpendicular to the flow. The precise fluid dynamic mechanisms which turn the ellipse were effectively realized for the first time in this simulation.

8. Feng, J., Hu, H. and Joseph, D.D., 1994, "Direct Simulation of Initial Value Problems for the Motion of Solid Bodies in a Newtonian Fluid. Part 2: Couette and Poiseuille Flows," *J. Fluid Mech.*, (in press).

This paper reports the results of a two-dimensional finite element simulation of the motion of a circular particle in a Couette and Poiseuille flow. The size of the particle and the Reynolds number are large enough to include fully non-linear inertial effects and wall effects. Both neutrally buoyant and non-neutrally buoyant particles are studied and the results are compared with pertinent experimental data and perturbation theories. A neutrally buoyant particle is shown to migrate to the centerline in a Couette flow, and exhibits the Segré-Silberberg effect in a Poiseuille flow. Non-neutrally buoyant particles have more complicated patterns of migration, depending upon the density difference between the fluid and the particle. The driving forces of the migration have been identified as a wall repulsion due to lubrication, an inertial lift related to shear-slip, a lift due to particle rotation, and in the case of Poiseuille flow, a lift caused by the velocity profile curvature. These forces are analyzed by interrogating the distributions of pressure and shear stress on the particle. The stagnation pressures on the particle surface are particularly important in determining the direction of migration.

9. Feng, J., Joseph, D.D., Glowinski, R. and Pan, T.W., 1993, "A Three-Dimensional Computation of the Force and Moment on an Ellipsoid Settling Slowly Through a Viscoelastic Fluid," *MSI Preprint* 93/217.

The orientation of an ellipsoid falling in a viscoelastic fluid filling a long cylinder of square cross-section is studied by methods of perturbation theory, with the added caveat that the perturbation problems are resolved without approximation by direct numerical simulation. Asymptotically, for small fall velocity, the fluid's rheology is described by a second-order fluid model. There are three problems: the zeroth order Stokes problem for a translating ellipsoid and two first order problems, one for inertia and one for second order rheology. A Stokes operator is inverted in each of the three cases. The problems are solved numerically on a three-dimensional domain by a finite element method with fictitious domains, and the force and moment on the body are evaluated. The results show that the signs of the perturbation pressure and velocity around the particle for inertia are reversed by viscoelasticity. The moments are also of opposite sign: inertia turns the major axis of the ellipsoid perpendicular to the fall; normal stresses turn the major axis parallel to fall. The competition of these two effects gives rise to an equilibrium tilt angle between perpendicular and parallel, which the settling ellipsoid would eventually assume. The equilibrium tilt angle is a function of the elasticity number, which is the ratio of the Weissenberg number and the Reynolds number. This ratio is velocity-independent and the theory is valid for small velocities. Very small *elasticity numbers are required to make the ellipsoid turn to a fixed angle of tilt between perpendicular and parallel. The results are in qualitative agreement with observations of shape tilting but they do not explain the sudden turning of a long body which occurs when a critical fall velocity is exceeded.*

The problem solved is described mathematically by the following equations (in dimensionless form)

$$\begin{cases} \nabla \cdot \mathbf{u} = 0 \\ \nabla p - \nabla^2 \mathbf{u} = -R(\mathbf{u} \cdot \nabla \mathbf{u}) - W\nabla \cdot \left(\mathbf{A}_2 + e\mathbf{A}_1^2\right) \\ \mathbf{u}\big|_g = \mathbf{e}_g \\ \mathbf{u}\big|_g = 0 \end{cases} \tag{2}$$

where p is the pressure, $\mathbf{u}$ is the velocity in a system of coordinates in which the ellipse is stationary and the sides of the rectangular channel move up with a unit velocity. R is a Reynolds number and W is a Weissenberg number. The coefficient of W represents the effects of normal stress. The problem is solved by perturbations

$$\begin{aligned} \mathbf{u} &= \mathbf{u}_0 + R\mathbf{u}_1 + W\mathbf{u}_2, \\ p &= p_0 + Rp_1 + Wp_2 \end{aligned} \tag{3}$$

where $\mathbf{u}_0$ and p_0 are a Stokes flow, $\mathbf{u}_1$ and p_1 are perturbations of Stokes flow with inertia and $\mathbf{u}_2$ and p_2 are perturbations of Stokes flow with normal stresses. The perturbation problems are generated in the usual way, but they are solved numerically.

A fictitious domain was used to solve these boundary value problems on multiply-connected domains. The basic idea is to convert the original problem into a new one posed on an auxiliary domain of a simple shape which contains the actual domain. Then structured mesh and fast solvers can be used on the auxiliary domain. The application of this method to incompressible viscous flows has been explored by Glowinski, Pan and Periaux [1993]. Sketches of $\mathbf{u}_0$, $\mathbf{u}_1$, $\mathbf{u}_2$, p_1 and p_2 are shown bn Figure 4 below, together with explanatory captions.

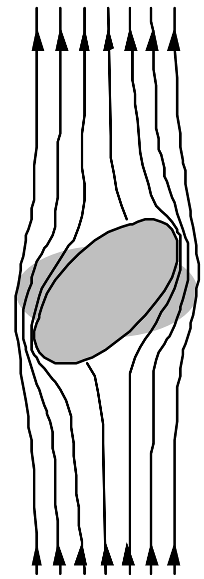

(a) Stokes flow $\mathbf{u}_0$.

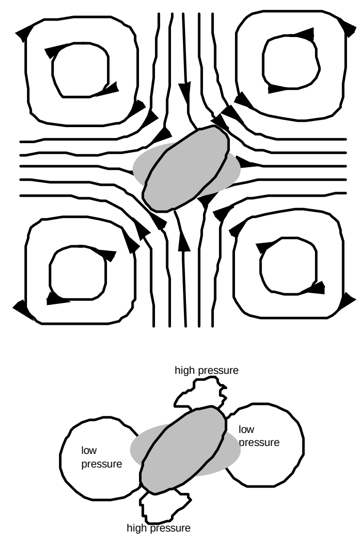

(b) Perturbation of Stokes flow with inertia, streamlines $\mathbf{u}_1$ and pressure p_1.

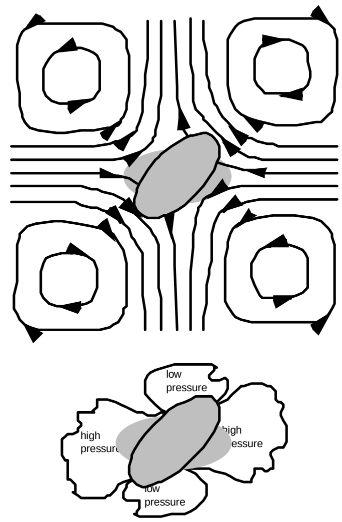

(c) Perturbation of Stokes flow with normal stresses, streamlines $\mathbf{u}_2$ and pressure p_2.

Figure 4. Perturbation of Stokes flow (a) in a long cylinder of square cross-section with inertia (b) and normal stresses (c). The Stokes flow (a) enters from the bottom and leaves from the top. The stagnation points in (a) locate the position of high pressure in (b) and low pressure in (c). The flows in (b) and (c) are symmetric in the sense that the flow is into both top and bottom points of stagnation in the inertial case (b) and just the opposite in the viscoelastic case (c). The flows go from high to low pressure.

10. Hu. H.H., 1994, "Motion of a Circular Cylinder in a Viscous Liquid Between Parallel Plates," *Theoretical and Computational Fluid Dynamics* (submitted).

The motion of a cylinder in a viscous fluid between a channel of two parallel walls is studied. It is found that when the cylinder is translating very closely along one of the channel walls, it always rotates in the direction opposite to that of contact rolling along the nearest wall. When the cylinder is away from the walls, its rotation depends on the Reynolds number of the flow. In this study, two numerical methods were used. One is for the unsteady motion of a sedimenting cylinder initially released from a position close to one of the channel walls, where the Navier-Stokes equations are used for the fluid and the Newton's equations of motion for the rigid cylinder. The other is for the steady flow in which a cylinder is placed at different locations in a uniform flow field, or equivalently a cylinder is moving in a quiescent fluid with a constant velocity. The flow field, the drag, the side force (lift) and the torque experienced by the cylinder are studied in detail. The effects of the cylinder location in the channel, the size of the channel relative to the cylinder diameter and the Reynolds number of the flow are examined. In the limit when the cylinder is translating very closely along one of the walls, the flow in the gap between the cylinder and the wall is solved analytically using the lubrication approximation, and the numerical solution in the other region is used to piece together the whole flow field.

This simulation is of the type given by Liu et al. [1993, number 5 in this list], but it is carried further, has more detailed results and focuses on the differences between the motion of a sphere and a cylinder moving along a vertical wall. When the gap is small, the sphere will turn as if falling on a dry wall, but a cylinder will turn the other way. The differences in the drag and torque on a cylinder are due to the fact that the gap between the sphere and the wall is three dimensional while the gap between the cylinder and wall is two dimensional. Since the back flow due to the lubrication pressure is much weaker for the sphere than for a cylinder, the torque on a sphere is mainly due to the shear of the fluid in the minimum gap region.

11. Joseph, D.D., Liu, Y.J. Poletto, M. and Feng. J., 1994, "Aggregation and Dispersion of Spheres Falling in Viscoelastic Liquids," *J. Non-Newtonian Fluid Mech.* (in press), and 1993 *MSI Preprint* 93/185.

This paper focuses on the settling of one sphere near another or near a wall. We find maximum differences between Newtonian and viscoelastic liquids, with repulsion between nearby bodies in the Newtonian case and attraction in the viscoelastic case. Side-by-side arrangements of sedimenting spheres are unstable in exactly the same way that broadside-on settling of long bodies is unstable at subcritical speeds in a viscoelastic fluid. The line of centers between the spheres rotates from across to along the stream as the spheres are sucked together. The resulting chain of two spheres is a long body which is stable when the line between centers is parallel to the fall, but this configuration breaks up at supercritical speeds in which inertia again dominates. To explain the orientation of particles in the subcritical case, we correlate the aggregative power of a viscoelastic fluid with the zero shear value of the coefficient of ratio of the first normal stress difference to the shear stress, and for exceptional cases we introduce the idea of the memory of shear-thinning leading to corridors of reduced viscosity.

We did a two-dimensional simulation of the motion of two circular particles sedimenting in a channel filled with Newtonian fluid. In our experiments, spheres dropped side-by-side in Newtonian liquids would begin to rotate and drift rapidly away from each other and after a short time reach an apparently steady state with definite angular velocity and a fixed stand-away distance with no further drift. In this simulation, a fixed stand-away distance with the line of centers perpendicular to the flow is not achieved. The side-by-side configuration, however, is very persistent as the following figure indicates.

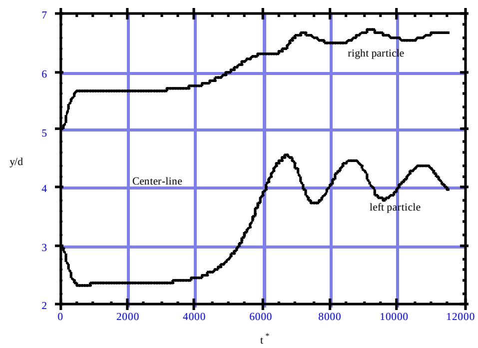

Figure 5. Trajectories of two circular cylinders dropped from a side-by-side initial condition in a channel of 8 diameters width. The dimensionless time is defined by $t^* = t\sqrt{g/d}$. The oscillation seen in the trajectories is associated with a wall effect.

At first, when the side-by-side particles are close together, the passage of fluid between the particles is blocked, so that the flow passes over the outside of the particle, turning them from the outside. We are going to show that the pressure and the shear stress distributions on the surface of the particle give rise to a lateral force and a torque that define the drift and rotation of the particle.

Figure 6 shows that the maximum pressure occurs near *q* = 202.5_. This position is also where the dividing streamline seems to hit the surface of the body. Because the circular particle is rotating, the no-slip condition implies that there are closed streamlines around the surface of the particle and a stagnation point cannot be strictly defined. The stagnation point usually corresponds to vanishing shear stress. This is not the case here because of the strong rotation of the particle. If we modify the shear stress by taking out the contribution from rotation, we should still have the correspondence. This is done by considering a potential vortex at the center of the particle with velocity

$$u_q^p = wa^2 / r \qquad (4)$$

where *w* is the angular velocity at this moment. The shear at *r* = *a* for this is

$$t_{rq}^p = -2hw \qquad (5)$$

Figure 6 shows that the extreme values of the pressure are near to the zeros of the effective shear stress.

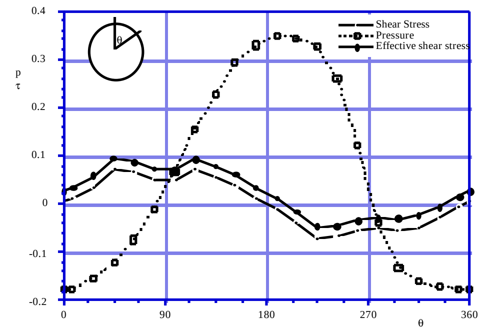

Figure 6. The pressure and shear stress distribution on the surface of the right particle. Dimensionless time $t^* = 31$ and instantaneous Reynolds number $R = 2.65$.

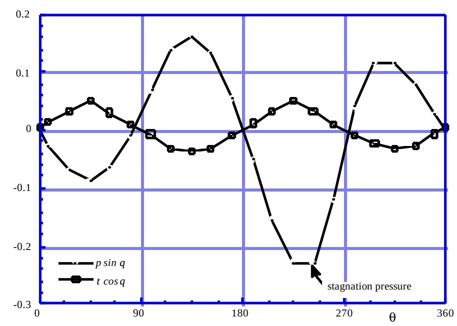

Figure 7. The horizontal component of the pressure and shear stress shown in Figure 6. Because of the definition of *q*, negative lateral thrusts point to the right.

The rotation of the particle is associated with the fact that the positive shear stress on the right side is larger than the negative shear stress on the left. Figure 7 shows that the stagnation pressure controls the sidewise drift, increasing the distance between repelling particles. In this figure, we have compared the side thrusts, *p* sin*q* of the pressure and τ cos*q* of the shear stress on the surface of the particle. The resultant forces are

$$\begin{aligned}\left[F_p, F_t\right] &= \int_0^{2p} [\, p \sin q,\ \ t \cos q \,] a dq \\ &= \left(1.602 \times 10^{-3},\ \ 8.034 \times 10^{-4}\right) \text{dyne/cm}\end{aligned} \qquad (6)$$

The pressure force is larger than the shear stress force, and the separation of the two particles is therefore determined mainly by stagnation pressure.

12. Feng. J., Huang, P.Y. and Joseph, D.D., 1994, "Dynamic Simulation of the Motion of Capsules in Pipelines," (in preparation).

In this paper we report results of two-dimensional simulations on the motion of elliptic capsules carried by a Poiseuille flow in a channel. The numerical methods allows dynamic computation of the capsule motion and the fluid flow around the capsule and accurate evaluation of the lift force and torque on it. Results show that the motion of a capsule heavier than the carrying fluid has three stages: initial lift-off, transient oscillations and steady flying. The behavior of the capsule during initial lift-off and steady flying is analyzed by studying the pressure and shear stress distributions on the capsule surface. The dominant mechanism for the lift force and torque is identified to be lubrication or inertia or a combination of the two under different conditions. Elliptic capsules seem to lift off more easily than cylindrical ones. Numerical results for the ellipse in two dimensions are compared with experimental observations of cylindrical capsules in pipes. Finally, the mechanisms of lift for capsules are applied to flying core flows, and it is argued that inertial forces are responsible for levitating heavy crude oil cores lubricated by water in a horizontal pipeline.

13. Hesla, T., Singh, P. and Joseph, D.D., 1994, "The Dynamical Simulation of Two-Dimensional Fluid/Particle Systems," (in preparation).

A new time-stepping finite-element scheme for the numerical simulation of two-dimensional fluid/particle systems is presented. The scheme is based on a variational equation governing the rate of change of total system momentum -- fluid plus particles. This equation incorporates both the Navier-Stokes and rigid-body equations and prevents numerical instability due to coupling between the fluid and particle momenta.

The efficacy of the new scheme is demonstrated by a series of benchmark tests in which a single heavy disk is dropped from rest in a channel of otherwise quiescent fluid, and the results are compared with experiments and with numerically computed drag coefficients.

The Navier-Stokes solver used in this simulation is based on the time-dependent code of Bristeau, Glowinski and Periaux [1987]. Among the problems treated is the problem of evolution to the equilibrium position of two circular particles in a Poiseuille flow. We find that the particles ultimately line up with the line of centers along the stream at a certain distance from the wall in agreement with experiments.

CONCLUDING REMARKS

It is our intention to develop numerical methods for direct simulations of particles in flows of viscoelastic fluids and in three dimensions. The force calculation of Feng, Joseph, Glowinski and Pan [1993] is our first effort in this direction. The motion of particles in viscoelastic fluids is not at all like the motions of particles in Newtonian fluids. In general, particles aggregate in viscoelastic fluids in situations in which they would disperse in Newtonian fluids. Long bodies which turn broadside-on in Newtonian fluids put their broadside parallel to the stream in viscoelastic fluids. One of the mechanisms which appears to work in producing these maximal differences between Newtonian and viscoelastic flows is a reversal of the pressure (actually, the normal stress) at a point of stagnation. However, this mechanism does not explain all of the observed features and more needs to be done.

ACKNOWLEDGEMENTS

This work was supported the NSF, Fluid, Particulate and Hydraulic Systems, by the U.S. Army, Mathematics and AHPCRC, by the DOE, Department of Basic Energy Sciences, the Minnesota Supercomputer Institute and the Schlumberger foundation.

REFERENCES

(References to papers in which I am an author are listed by number in the text under 'Selected Works' and will not be repeated here.)

Bristeau, M.O., Glowinski, R. and Periaux, J., 1987, "Numerical Methods for the Navier-Stokes Equations. Applications to the Simulation of Compressible and Incompressible Flows," *Comput. Phys. Rep.* **6**, pp. 73-187.

Crochet, M.J., Debaut, B., Keunings, R. and Marchal, J.M., 1991, "POLYFLOW: A Finite Element Program for Modelling Processes," in *CAE for Polymer Processing: Applications in Extrusions and Other Continuous Processes*, (ed. O'Brian), Hansen Publishers.

Hecht, F. and Saltel, E., 1989, "EMC2 un logiciel d'edition de maillages et de contours bidimensionels, Rapport, INRIA.

Glowinski, R., Pan, T.W. and Periaux, J., 1993, "A Fictitious Domain Method for External Incompressible Viscous Flow Modeled by Navier-Stokes Equations," *Comput. Methods in Appl. Mech and Engng*, (to appear).